

Energy decomposition analysis based on broken symmetry unrestricted density functional theory

Cite as: J. Chem. Phys. **151**, 244106 (2019); <https://doi.org/10.1063/1.5114611>

Submitted: 11 June 2019 • Accepted: 03 December 2019 • Published Online: 23 December 2019

 Zhen Tang, Zhen Jiang, Hongjiang Chen, et al.



View Online



Export Citation



CrossMark

ARTICLES YOU MAY BE INTERESTED IN

[A consistent and accurate ab initio parametrization of density functional dispersion correction \(DFT-D\) for the 94 elements H-Pu](#)

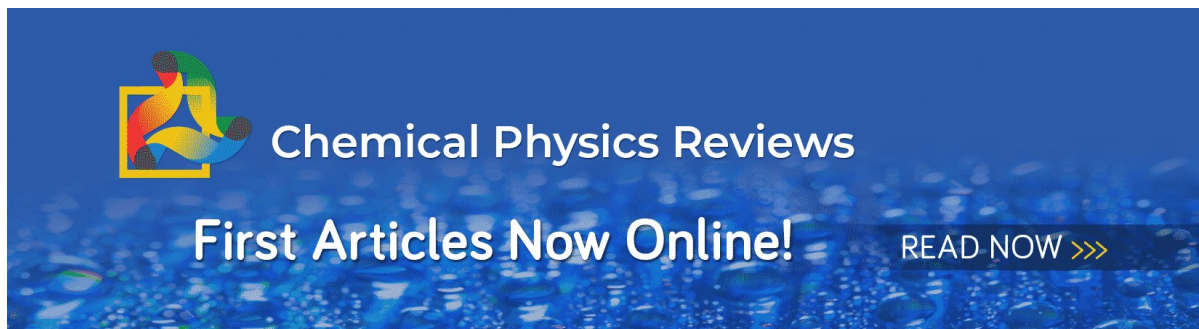
The Journal of Chemical Physics **132**, 154104 (2010); <https://doi.org/10.1063/1.3382344>

[Energy decomposition analysis of covalent bonds and intermolecular interactions](#)

The Journal of Chemical Physics **131**, 014102 (2009); <https://doi.org/10.1063/1.3159673>

[The ORCA quantum chemistry program package](#)

The Journal of Chemical Physics **152**, 224108 (2020); <https://doi.org/10.1063/5.0004608>



Chemical Physics Reviews

First Articles Now Online!

READ NOW >>>

Energy decomposition analysis based on broken symmetry unrestricted density functional theory

Cite as: J. Chem. Phys. 151, 244106 (2019); doi: 10.1063/1.5114611

Submitted: 11 June 2019 • Accepted: 3 December 2019 •

Published Online: 23 December 2019



View Online



Export Citation



CrossMark

Zhen Tang, Zhen Jiang, Hongjiang Chen, Peifeng Su,^{a)} and Wei Wu

AFFILIATIONS

Fujian Provincial Key Laboratory of Theoretical and Computational Chemistry, The State Key Laboratory of Physical Chemistry of Solid Surfaces, and College of Chemistry and Chemical Engineering, Xiamen University, Xiamen 361005, China

^{a)}Author to whom correspondence should be addressed: supi@xmu.edu.cn

ABSTRACT

In this paper, the generalized Kohn-Sham energy decomposition analysis (GKS-EDA) scheme is extended to molecular interactions in open shell singlet states, which is a challenge for many popular EDA methods due to the multireference character. Based on broken symmetry (BS) unrestricted density functional theory with a spin projection approximation, the extension scheme, named GKS-EDA(BS) in this paper, divides the total interaction energy into electrostatic, exchange-repulsion, polarization, correlation, and dispersion terms. Test examples include the pancake bond in the phenalenyl dimer, the ligand interactions in the Fe(II)-porphyrin complexes, and the radical interactions in dehydrogenated guanine-cytosine base pairs and show that GKS-EDA(BS) is a practical EDA tool for open shell singlet systems.

Published under license by AIP Publishing. <https://doi.org/10.1063/1.5114611>

I. INTRODUCTION

Energy decomposition analysis (EDA) is an important quantitative analysis approach for intermolecular interactions based on electronic structure calculations. Many popular EDA methods are based on Hartree-Fock (HF) or Kohn-Sham-density functional theory (KS-DFT) orbitals.^{1–16} They have been fruitfully applied to various chemical problems, including noncovalent interactions, covalent bonds, chemical reactions, force field developments, and so on. These schemes include Kitaura–Morokuma (KM) EDA,^{1,2} extended transition state/extended transition state with natural orbitals for chemical valence (ETS/ETS-NOCV) EDA,^{3,12} constrained space orbital variation (CSOV) EDA,⁴ symmetry-adapted perturbation theory (SAPT),^{5,6} reduced variational space (RVS) EDA,⁷ block-localized wavefunction (BLW) EDA,⁹ absolutely localized molecular orbital (ALMO) EDA,¹¹ localized molecular orbital (LMO) EDA,^{13,15} etc. Recently, we proposed the generalized Kohn-Sham energy decomposition analysis (GKS-EDA) scheme based on LMO-EDA and generalized Kohn-Sham theory.¹⁶ By utilizing various DFT functionals, GKS-EDA performs interaction analysis for open shell [with high spins (HSs)] and closed shell systems. Moreover, by using a fragmentation scheme, the GKS-EDA method has been extended to the analysis for intramolecular interactions in the gas

phase and solution phase.^{17,18} The method has been applied to various chemical problems,^{19–36} showing its robustness and potential capability.

Intermolecular interactions in molecular systems with open shell singlet (OSS) states, such as magnetic interactions, transit metal-ligand bonding, and π - π radical stacking, become more and more important in biochemistry, photophysics, material science, etc.^{37,38} In the OSS molecular systems, the frontier molecular orbitals of the interacting systems are near-degenerate. Due to multireference characters, the theoretical analysis for OSS type molecular interactions is one of the challenges to the single configuration based EDA methods.³⁹ It is noticed that several efforts have been devoted to develop new EDA methods for intermolecular interactions in OSS states. For example, Patkowski *et al.* proposed a new extension of SAPT, called the first order spin-flip SAPT.^{40,41} This work paves the way for SAPT to analyze weak intermolecular interactions in arbitrary spin states.

A reliable quantum chemical description of OSS systems can be provided by multiconfiguration/multireference methods. In the 1980s, an MCSCF based EDA scheme was proposed by Bernardi and Robb.⁴² The scheme divides the total interaction energy into the sum of electrostatic and exchange repulsion and valence charge transfer, the sum of orbital polarization and charge transfer, and

configuration interaction terms. It was applied to the rotational barrier in ethane, the dimerization of methylene, the reaction of methylene and silylene, etc. After then, several EDA schemes based on multireference wave function have been proposed.^{43–47} Suffering from the expensive computational cost, multireference wave function based EDA methods are very difficult if not possible to be applied to large or medium size systems.

Besides multireference methods, an alternative approach for the OSS type interactions is broken symmetry unrestricted density functional theory (BS-UDFT).^{48,49} Combined with a spin projection approximation, BS-UDFT describes the energy of the ground state (GS) through a linear combination of two independent energy calculations of the unrestricted spin configurations, i.e., broken-symmetry (BS) state and high-spin (HS) state.^{50,51} BS-UDFT has been employed in the theoretical descriptions for molecular systems of open shell singlet states.^{52–55} For example, based on BS-UDFT, Malrieu *et al.* present an analysis procedure to calculate the various components of the magnetic couplings in diradicals.^{53,54} In the ALMO-EDA scheme developed by Head-Gordon *et al.*, a broken symmetry technique is used to consider the spin coupling term in the analysis of a single covalent bond.⁵⁵

The motivation of this paper is to present an extension of GKS-EDA to intermolecular interactions in open shell singlet states. The extension scheme is based on broken symmetry unrestricted density functional theory, thus named GKS-EDA(BS) in this paper, and is designed for the general use both in the gas phase and in the solution phase. It should be noted that the performance of BS-UDFT depends on the choice of the functional. Pure DFT functionals do not work well with the broken symmetry scheme.⁵⁴ In this paper, a series of hybrid and range-separated hybrid functionals are employed for GKS-EDA(BS) calculations. The selected applications in this paper include the π - π radical interaction, transit-metal ligand bonding, and interactions in dehydrogenated based pairs, covering the interactions in organic materials, metalloproteins, and biomolecules, respectively.

II. METHODOLOGY

A. GKS-EDA

Density functional theory (DFT) is a powerful and efficient method for many-electron systems.⁵⁶ DFT is based on the Hohenberg-Kohn theorem,⁵⁷ which states that there exists a one-to-one correspondence between the electron density of a system and the energy. In practice, the overwhelming majority of DFT applications are attributed to the Kohn-Sham DFT (KS-DFT) scheme.^{56,58} KS-DFT maps a many-electron system into a noninteracting electron system that yields the same ground state density. In KS-DFT, the exchange-correlation functional describes the nonclassical part of the electron-electron interaction. The exchange-correlation functional is inherently local because it depends on electron density only.

The generalized Kohn-Sham (GKS) scheme maps the real system to a partially interacting model system, which can be represented by a single Slater determinant.⁵⁹ In the GKS scheme, not only the noninteracting kinetic energy but also the part of electron-electron interaction is treated exactly. In the

Hartree-Fock-Kohn-Sham form of the GKS scheme, electronic density ρ is achieved from the Kohn-Sham orbitals $\{\phi_i\}$ computed by the following equations:

$$(h + v_I + v_X^{\text{HF}} + v_C^{\text{GKS}})|\phi_i\rangle = \varepsilon_i|\phi_i\rangle, \quad (1)$$

$$v_C^{\text{GKS}} = (1 - a)(v_X(\rho) - v_X^{\text{HF}}) + v_C(\rho), \quad (2)$$

where h is the one electron operator for the sum of kinetic and nuclear-electron potential, v_I and v_X^{HF} are the Coulomb operator and exchange operator, respectively, $v_X(\rho)$ and $v_C(\rho)$ are the exchange and correlation potential, respectively, and a is the portion of the exact HF energy, ranging from 0 to 1. Thereafter, not only local functionals but also nonlocal functionals, including hybrid, double hybrid, and range-separated functionals, etc., can be treated by the generalized Kohn-Sham (GKS) scheme.

Using the Kohn-Sham spin orbitals $\{\phi_i\}$, the total energy can be expressed as

$$\begin{aligned} E = & \sum_i^{\alpha, \beta} \langle i | h | i \rangle + \frac{1}{2} \sum_i^{\alpha, \beta} \sum_j^{\alpha, \beta} \langle ij | ij \rangle - \frac{1}{2} \left(\sum_i^{\alpha} \sum_j^{\alpha} \langle ij | ji \rangle + \sum_i^{\beta} \sum_j^{\beta} \langle ij | ji \rangle \right) \\ & + E^{\text{nuc}} + (1 - a) \left[E_X(\rho^\alpha, \rho^\beta) + \frac{1}{2} \left(\sum_i^{\alpha} \sum_j^{\alpha} \langle ij | ji \rangle + \sum_i^{\beta} \sum_j^{\beta} \langle ij | ji \rangle \right) \right] \\ & + E_C(\rho^\alpha, \rho^\beta), \end{aligned} \quad (3)$$

where E^{nuc} is the nuclear repulsion energy, i and j denote all the occupied α and β spin orbitals, and $E_X(\rho^\alpha, \rho^\beta)$ and $E_C(\rho^\alpha, \rho^\beta)$ are the exchange and correlation energy of a DFT functional with the α and β spin density. If a double hybrid functional, e.g., B2PLYP, is applied, $E_C(\rho^\alpha, \rho^\beta)$ is replaced by $(1 - C_{\text{MP2}})E_C(\rho^\alpha, \rho^\beta) + C_{\text{MP2}}\Delta E_{\text{MP2}}$, where ΔE_{MP2} is the MP2 correlation energy from KS orbitals with the amount accounted by C_{MP2} .

Based on the generalized Kohn-Sham (GKS) scheme,⁵⁹ GKS-EDA divides the total interaction energy into electrostatic (ΔE^{ele}), exchange-repulsion (ΔE^{exrep}), polarization (ΔE^{pol}), correlation (ΔE^{corr}), and dispersion (ΔE^{disp}) terms¹⁶ as follows:

$$\Delta E^{\text{TOT}} = \Delta E^{\text{ele}} + \Delta E^{\text{exrep}} + \Delta E^{\text{pol}} + \Delta E^{\text{corr}} + \Delta E^{\text{disp}}, \quad (4)$$

where the individual terms are defined as

$$\begin{aligned} \Delta E^{\text{ele}} = & \sum_{i \in \phi_0}^{\alpha, \beta} \langle i | h | i \rangle + \frac{1}{2} \sum_{i \in \phi_0}^{\alpha, \beta} \sum_{j \in \phi_0}^{\alpha, \beta} \langle ij | ij \rangle + E_S^{\text{nuc}} \\ & - \sum_A \left(\sum_{i \in \phi_A}^{\alpha, \beta} \langle i | h | i \rangle + \frac{1}{2} \sum_{i \in \phi_A}^{\alpha, \beta} \sum_{j \in \phi_A}^{\alpha, \beta} \langle ij | ij \rangle + E_A^{\text{nuc}} \right), \end{aligned} \quad (5)$$

where ϕ_0 is the direct product of monomers' wave function and ϕ_A is the wave function of monomer A,

$$\Delta E^{\text{exrep}} = \Delta E^{\text{ex}} + \Delta E^{\text{rep}}, \quad (6)$$

where ΔE^{ex} and ΔE^{rep} can be defined as

$$\Delta E^{\text{ex}} = -\frac{1}{2} \sum_{\text{A}} \left(\sum_{i \in \phi_{\text{A}}}^{\alpha} \sum_{j \notin \phi_{\text{A}}}^{\beta} \langle ij | ji \rangle + \sum_{i \in \phi_{\text{A}}}^{\beta} \sum_{j \notin \phi_{\text{A}}}^{\alpha} \langle ij | ji \rangle \right) \quad (7)$$

and

$$\begin{aligned} \Delta E^{\text{rep}} = & \sum_{i \in \phi_0}^{\alpha} \sum_{j \in \phi_0}^{\beta} \langle i | h | j \rangle (S_{ij}^{-1} - \delta_{ij}) + \frac{1}{2} \sum_{i \in \phi_0}^{\alpha} \sum_{j \in \phi_0}^{\beta} \sum_{k \in \phi_0}^{\alpha} \sum_{l \in \phi_0}^{\beta} \langle ij | kl \rangle (S_{ik}^{-1} S_{jl}^{-1} - \delta_{ik} \delta_{jl}) \\ & - \frac{1}{2} \left[\sum_{i \in \phi_0}^{\alpha} \sum_{j \in \phi_0}^{\alpha} \sum_{k \in \phi_0}^{\alpha} \sum_{l \in \phi_0}^{\alpha} \langle ij | lk \rangle (S_{il}^{-1} S_{jk}^{-1} - \delta_{il} \delta_{jk}) + \sum_{i \in \phi_0}^{\beta} \sum_{j \in \phi_0}^{\beta} \sum_{k \in \phi_0}^{\beta} \sum_{l \in \phi_0}^{\beta} \langle ij | lk \rangle (S_{il}^{-1} S_{jk}^{-1} - \delta_{il} \delta_{jk}) \right], \end{aligned} \quad (8)$$

respectively.

$$\begin{aligned} \Delta E^{\text{pol}} = & \sum_{i \in \phi_{\text{S}}}^{\alpha} \langle i | h | i \rangle + \frac{1}{2} \sum_{i \in \phi_{\text{S}}}^{\alpha} \sum_{j \in \phi_{\text{S}}}^{\beta} \langle ij | ij \rangle - \frac{1}{2} \left(\sum_{i \in \phi_{\text{S}}}^{\alpha} \sum_{j \in \phi_{\text{S}}}^{\alpha} \langle ij | ji \rangle + \sum_{i \in \phi_{\text{S}}}^{\beta} \sum_{j \in \phi_{\text{S}}}^{\beta} \langle ij | ji \rangle \right) \\ & - \left[\sum_{i \in \phi_0}^{\alpha} \sum_{j \in \phi_0}^{\beta} \langle i | h | j \rangle S_{ij}^{-1} + \frac{1}{2} \sum_{i \in \phi_0}^{\alpha} \sum_{j \in \phi_0}^{\beta} \sum_{k \in \phi_0}^{\alpha} \sum_{l \in \phi_0}^{\beta} \langle ij | kl \rangle S_{ik}^{-1} S_{jl}^{-1} \right. \\ & \left. - \frac{1}{2} \left(\sum_{i \in \phi_0}^{\alpha} \sum_{j \in \phi_0}^{\alpha} \sum_{k \in \phi_0}^{\alpha} \sum_{l \in \phi_0}^{\alpha} \langle ij | lk \rangle S_{il}^{-1} S_{jk}^{-1} + \sum_{i \in \phi_0}^{\beta} \sum_{j \in \phi_0}^{\beta} \sum_{k \in \phi_0}^{\beta} \sum_{l \in \phi_0}^{\beta} \langle ij | lk \rangle S_{il}^{-1} S_{jk}^{-1} \right) \right], \end{aligned} \quad (9)$$

where ϕ_{S} is the supermolecule's wave function.

$$\begin{aligned} \Delta E^{\text{corr}} = & (1 - a) \left[E_{\text{X}}(\rho_{\text{S}}^{\alpha}, \rho_{\text{S}}^{\beta}) + \frac{1}{2} \left(\sum_{i \in \phi_{\text{S}}}^{\alpha} \sum_{j \in \phi_{\text{S}}}^{\alpha} \langle ij | ji \rangle + \sum_{i \in \phi_{\text{S}}}^{\beta} \sum_{j \in \phi_{\text{S}}}^{\beta} \langle ij | ji \rangle \right) \right] + E_{\text{C}}(\rho_{\text{S}}^{\alpha}, \rho_{\text{S}}^{\beta}) \\ & - \sum_{\text{A}} \left[(1 - a) \left[E_{\text{X}}(\rho_{\text{A}}^{\alpha}, \rho_{\text{A}}^{\beta}) + \frac{1}{2} \left(\sum_{i \in \phi_{\text{A}}}^{\alpha} \sum_{j \in \phi_{\text{A}}}^{\alpha} \langle ij | ji \rangle + \sum_{i \in \phi_{\text{A}}}^{\beta} \sum_{j \in \phi_{\text{A}}}^{\beta} \langle ij | ji \rangle \right) \right] + E_{\text{C}}(\rho_{\text{A}}^{\alpha}, \rho_{\text{A}}^{\beta}) \right], \end{aligned} \quad (10)$$

$$\Delta E^{\text{disp}} = E_{\text{S}}^{\text{disp}} - \sum_{\text{A}} E_{\text{A}}^{\text{disp}}. \quad (11)$$

In the above equations, (5)–(11), S and A denote the supermolecule and the monomer, respectively. ΔE^{disp} in Eq. (11) is optional for dispersion correction DFT, such as Grimme's dispersion functionals,⁶⁰ defined as the difference between dispersion corrections of the supermolecule ($E_{\text{S}}^{\text{disp}}$) and of monomer ($E_{\text{A}}^{\text{disp}}$). It is stressed that the dispersion term is not spin-dependent.

For molecular interactions in the solution phase, GKS-EDA employs implicit solvation models [conductor-like polarizable continuum model (CPCM),^{61,62} integral equation formulation of polarizable continuum model (IEPCM),^{63–66} and so on] to take the influence of long range solvent effects into account. The total interaction free energy is expressed as

$$\Delta G^{\text{TOT}} = \Delta G^{\text{ele}} + \Delta G^{\text{exrep}} + \Delta G^{\text{pol}} + \Delta G^{\text{corr}} + \Delta G^{\text{disp}} + \Delta G^{\text{desol}}, \quad (12)$$

where the first five terms are the same as the corresponding terms in Eq. (4) except that the orbitals used in these terms are optimized by the self-consistent reaction field (SCRF) in implicit solvation models.

The final term in Eq. (13), ΔG^{desol} , which denotes the energy penalty by solvent environments, is computed by the implicit solvation model as

$$\Delta G^{\text{desol}} = \frac{1}{2} \nu_{\text{S}}^{\text{SOL}} \cdot q_{\text{S}} - \sum_{\text{A}} \frac{1}{2} \nu_{\text{A}}^{\text{SOL}} \cdot q_{\text{A}}, \quad (13)$$

where ν^{SOL} is the reaction field operator and q_{S} and q_{A} denote the induced surface charges that distribute on the set of tesserae on the cavities of the supermolecule S and monomer A, respectively. The induced surface charges and the reaction field operator are determined by the PCM method^{61–66} and the tesserae scheme.⁶⁷

B. GKS-EDA(BS)

In the broken symmetry unrestricted density functional theory (BS-UDFT), opposite spin electrons locate at different KS orbitals that allowed to polarize. Because unrestricted Kohn-Sham orbitals

are not eigenfunctions of the spin operator S^2 , the use of spin decontamination schemes is required. Various schemes have been presented to address the problem of the spin contamination.^{48,68–82} Among them, the spin projection approximation^{48,71,72,74,75,77} is simple and widely used.

In the spin projection approximation proposed by Yamaguchi and co-workers,^{72,74,75} the ground state (GS) energy can be expressed as

$$E_{\text{GS}} = (1 + c)E_{\text{BS}} - cE_{\text{HS}}, \quad (14)$$

where E_{BS} and E_{HS} are the total energies in the broken symmetry (BS) singlet state and high spin (HS) state, respectively. c is defined as

$$c = \frac{\langle \hat{S}^2 \rangle_{\text{BS}}}{\langle \hat{S}^2 \rangle_{\text{HS}} - \langle \hat{S}^2 \rangle_{\text{BS}}}. \quad (15)$$

Accordingly, the total interaction energy at the ground state of the interacting system is expressed as

$$\Delta E_{\text{GS}}^{\text{TOT}} = (1 + c)\Delta E_{\text{BS}}^{\text{TOT}} - c\Delta E_{\text{HS}}^{\text{TOT}}, \quad (16)$$

where $\Delta E_{\text{BS}}^{\text{TOT}}$ and $\Delta E_{\text{HS}}^{\text{TOT}}$ are the total interaction energies in the BS state and HS state, respectively, defined as

$$\Delta E_{\text{BS}}^{\text{TOT}} = E_{\text{BS}} - E_{\text{A}} - E_{\text{B}}, \quad (17)$$

$$\Delta E_{\text{HS}}^{\text{TOT}} = E_{\text{HS}} - E_{\text{A}} - E_{\text{B}}. \quad (18)$$

It is noticed that the total interaction energies in both the BS state and HS state are spin-contaminated. However, as pointed out by Handy *et al.*,⁸³ spin contamination in HS states by using KS-DFT is usually weak. As such, the neglect of the spin contamination in the HS state is appropriate.

As can be seen, $\Delta E_{\text{GS}}^{\text{TOT}}$ is a linear combination of total interaction energies in the HS state and the BS state. For the strong coupling between the monomers ($c = 0$), the total interaction energy will retreat to the close shell interaction.

The interaction energy at a high spin state, $\Delta E_{\text{HS}}^{\text{TOT}}$, can be easily computed by a GKS-EDA calculation with parallel spins of monomers. For example, if HS is a triplet state (TS), it is assumed that each monomer shares one α electron. In a similar fashion to the regular GKS-EDA, $\Delta E_{\text{HS}}^{\text{TOT}}$ is decomposed as

$$\Delta E_{\text{HS}}^{\text{TOT}} = \Delta E_{\text{HS}}^{\text{ele}} + \Delta E_{\text{HS}}^{\text{exrep}} + \Delta E_{\text{HS}}^{\text{pol}} + \Delta E_{\text{HS}}^{\text{corr}} + \Delta E_{\text{HS}}^{\text{disp}}. \quad (19)$$

To compute $\Delta E_{\text{BS}}^{\text{TOT}}$, the broken symmetry form ϕ_0^{BS} is constructed from the direct product of the monomers' wave function. It is noted that unpaired electrons with different spins locate at different monomers. For example, for the interacting system in an open shell singlet state with two unpaired electrons, the α electron locates at monomer A, while the β electron is in monomer B.

$\Delta E_{\text{BS}}^{\text{TOT}}$ is decomposed as

$$\Delta E_{\text{BS}}^{\text{TOT}} = \Delta E_{\text{BS}}^{\text{ele}} + \Delta E_{\text{BS}}^{\text{exrep}} + \Delta E_{\text{BS}}^{\text{pol}} + \Delta E_{\text{BS}}^{\text{corr}} + \Delta E_{\text{BS}}^{\text{disp}}. \quad (20)$$

$\Delta E_{\text{BS}}^{\text{ele}}$ is defined as

$$\Delta E_{\text{BS}}^{\text{ele}} = \sum_{i \in \phi_0^{\text{BS}}}^{\alpha, \beta} \langle i | h | i \rangle + \frac{1}{2} \sum_{i \in \phi_0^{\text{BS}}}^{\alpha, \beta} \sum_{j \in \phi_0^{\text{BS}}}^{\alpha, \beta} \langle ij | ij \rangle + E_{\text{S}}^{\text{nuc}} - \sum_{\text{A}} \left(\sum_{i \in \phi_{\text{A}}}^{\alpha, \beta} \langle i | h | i \rangle + \frac{1}{2} \sum_{i \in \phi_{\text{A}}}^{\alpha, \beta} \sum_{j \in \phi_{\text{A}}}^{\alpha, \beta} \langle ij | ij \rangle + E_{\text{A}}^{\text{nuc}} \right), \quad (21)$$

$$\Delta E_{\text{BS}}^{\text{exrep}} = \Delta E_{\text{BS}}^{\text{ex}} + \Delta E_{\text{BS}}^{\text{rep}}. \quad (22)$$

The definition of $\Delta E_{\text{BS}}^{\text{ex}}$ is the same as that of ΔE^{ex} , while $\Delta E_{\text{BS}}^{\text{rep}}$ can be defined as

$$\begin{aligned} \Delta E_{\text{BS}}^{\text{rep}} = & \sum_{i \in \phi_0^{\text{BS}}}^{\alpha, \beta} \sum_{j \in \phi_0^{\text{BS}}}^{\alpha, \beta} \langle i | h | j \rangle (S_{ij}^{-1} - \delta_{ij}) + \frac{1}{2} \sum_{i \in \phi_0^{\text{BS}}}^{\alpha, \beta} \sum_{j \in \phi_0^{\text{BS}}}^{\alpha, \beta} \sum_{k \in \phi_0^{\text{BS}}}^{\alpha, \beta} \sum_{l \in \phi_0^{\text{BS}}}^{\alpha, \beta} \langle ij | kl \rangle (S_{ik}^{-1} S_{jl}^{-1} - \delta_{ik} \delta_{jl}) \\ & - \frac{1}{2} \left[\sum_{i \in \phi_0^{\text{BS}}}^{\alpha} \sum_{j \in \phi_0^{\text{BS}}}^{\alpha} \sum_{k \in \phi_0^{\text{BS}}}^{\alpha} \sum_{l \in \phi_0^{\text{BS}}}^{\alpha} \langle ij | lk \rangle (S_{il}^{-1} S_{jk}^{-1} - \delta_{il} \delta_{jk}) + \sum_{i \in \phi_0^{\text{BS}}}^{\beta} \sum_{j \in \phi_0^{\text{BS}}}^{\beta} \sum_{k \in \phi_0^{\text{BS}}}^{\beta} \sum_{l \in \phi_0^{\text{BS}}}^{\beta} \langle ij | lk \rangle (S_{il}^{-1} S_{jk}^{-1} - \delta_{il} \delta_{jk}) \right], \end{aligned} \quad (23)$$

$$\begin{aligned} \Delta E_{\text{BS}}^{\text{pol}} = & \sum_{i \in \phi_0^{\text{BS}}}^{\alpha, \beta} \langle i | h | i \rangle + \frac{1}{2} \sum_{i \in \phi_0^{\text{BS}}}^{\alpha, \beta} \sum_{j \in \phi_0^{\text{BS}}}^{\alpha, \beta} \langle ij | ij \rangle - \frac{1}{2} \left(\sum_{i \in \phi_0^{\text{BS}}}^{\alpha} \sum_{j \in \phi_0^{\text{BS}}}^{\alpha} \langle ij | ji \rangle + \sum_{i \in \phi_0^{\text{BS}}}^{\beta} \sum_{j \in \phi_0^{\text{BS}}}^{\beta} \langle ij | ji \rangle \right) \\ & - \left[\sum_{i \in \phi_0^{\text{BS}}}^{\alpha, \beta} \sum_{j \in \phi_0^{\text{BS}}}^{\alpha, \beta} \langle i | h | j \rangle S_{ij}^{-1} + \frac{1}{2} \sum_{i \in \phi_0^{\text{BS}}}^{\alpha, \beta} \sum_{j \in \phi_0^{\text{BS}}}^{\alpha, \beta} \sum_{k \in \phi_0^{\text{BS}}}^{\alpha, \beta} \sum_{l \in \phi_0^{\text{BS}}}^{\alpha, \beta} \langle ij | kl \rangle S_{ik}^{-1} S_{jl}^{-1} \right. \\ & \left. - \frac{1}{2} \left(\sum_{i \in \phi_0^{\text{BS}}}^{\alpha} \sum_{j \in \phi_0^{\text{BS}}}^{\alpha} \sum_{k \in \phi_0^{\text{BS}}}^{\alpha} \sum_{l \in \phi_0^{\text{BS}}}^{\alpha} \langle ij | lk \rangle S_{il}^{-1} S_{jk}^{-1} + \sum_{i \in \phi_0^{\text{BS}}}^{\beta} \sum_{j \in \phi_0^{\text{BS}}}^{\beta} \sum_{k \in \phi_0^{\text{BS}}}^{\beta} \sum_{l \in \phi_0^{\text{BS}}}^{\beta} \langle ij | lk \rangle S_{il}^{-1} S_{jk}^{-1} \right) \right], \end{aligned} \quad (24)$$

where ϕ_S^{BS} is the supermolecule's wave function optimized by the SCF procedure of BS-UDFT. In the BS-UDFT calculations, ϕ_0^{BS} is set as the initial guess.

$\Delta E_{\text{BS}}^{\text{corr}}$ is defined as

$$\begin{aligned} \Delta E^{\text{corr}} = & (1-a) \left[E_X(\rho_S^\alpha, \rho_S^\beta) + \frac{1}{2} \left(\sum_{i \in \phi_S^{\text{BS}}}^{\alpha} \sum_{j \in \phi_S^{\text{BS}}}^{\alpha} \langle ij | ji \rangle + \sum_{i \in \phi_S^{\text{BS}}}^{\beta} \sum_{j \in \phi_S^{\text{BS}}}^{\beta} \langle ij | ji \rangle \right) \right] + E_C(\rho_S^\alpha, \rho_S^\beta) \\ & - \sum_A \left[(1-a) \left[E_X(\rho_A^\alpha, \rho_A^\beta) + \frac{1}{2} \left(\sum_{i \in \phi_A}^{\alpha} \sum_{j \in \phi_A}^{\alpha} \langle ij | ji \rangle + \sum_{i \in \phi_A}^{\beta} \sum_{j \in \phi_A}^{\beta} \langle ij | ji \rangle \right) \right] + E_C(\rho_A^\alpha, \rho_A^\beta) \right]. \end{aligned} \quad (25)$$

Finally, the definition of $\Delta E_{\text{BS}}^{\text{disp}}$ is the same as that of ΔE^{disp} because it does not depend on the wave function.

Therefore, the total interaction energy in the open shell singlet state is decomposed as

$$\Delta E_{\text{GS}}^{\text{TOT}} = \Delta E_{\text{GS}}^{\text{ele}} + \Delta E_{\text{GS}}^{\text{exrep}} + \Delta E_{\text{GS}}^{\text{pol}} + \Delta E_{\text{GS}}^{\text{corr}} + \Delta E_{\text{GS}}^{\text{disp}}. \quad (26)$$

Here,

$$\Delta E_{\text{GS}}^X = (1+c)\Delta E_{\text{BS}}^X - c\Delta E_{\text{HS}}^X. \quad (27)$$

Here, X can be electrostatic, exchange-repulsion, polarization, correlation, and dispersion, respectively. If $c=0$, these definitions will reduce to the regular GKS-EDA formulas.

The procedure of GKS-EDA(BS) is summarized as follows:

- (1) The supermolecule is divided into two monomers A and B. The unpaired α and β electrons are assigned to monomers A and B, respectively.
- (2) Let the spins of the two monomers be parallel. GKS-EDA calculation is performed at the HS state. Then, $\Delta E_{\text{HS}}^{\text{TOT}}$ and the interaction terms are computed.
- (3) Let different spins be located at different monomers. Initial broken symmetry wave function is constructed based on the KS-UDFT orbitals of monomers A and B. GKS-EDA(BS) calculation is carried out to gain $\Delta E_{\text{BS}}^{\text{TOT}}$ and the interaction terms in the BS state.
- (4) By using Eqs. (26) and (27), the total interaction energy $\Delta E_{\text{GS}}^{\text{TOT}}$ and the interaction terms are obtained.

If solvent effects are considered, the total interaction energy is expressed as

$$\Delta G_{\text{GS}}^{\text{TOT}} = \Delta G_{\text{GS}}^{\text{ele}} + \Delta G_{\text{GS}}^{\text{exrep}} + \Delta G_{\text{GS}}^{\text{pol}} + \Delta G_{\text{GS}}^{\text{corr}} + \Delta G_{\text{GS}}^{\text{disp}} + \Delta G_{\text{GS}}^{\text{desol}}, \quad (28)$$

where the desolvation term can be easily defined using Eqs. (13) and (27).

III. COMPUTATIONAL DETAILS

The modified GKS-EDA code is implemented in a home version of the General Atomic and Molecular Electronic Structure System (GAMESS).⁸⁴ All GKS-EDA computations are carried out by the GAMESS program.⁸⁴ The counterpoise (CP) method is applied for the basis set superposition error (BSSE) without dispersion

correction.⁸⁵ A series of hybrid DFT functionals, including B3LYP,⁸⁶ ω B97X-D,⁸⁷ TPSSh,⁸⁸ M05-2X,⁸⁹ and M06-2X,⁹⁰ are used. All the geometries are optimized by broken symmetry UDFT with the Gaussian 09 package.⁹¹ NBO analysis is performed by the NBO module in Gaussian 09 (version 3.1).⁹² CPCM is used to consider the implicit solvent effect.^{61,62} The universal force field radius model scaled by a factor of 1.1 is employed for CPCM calculations.⁹³

Test examples include the pancake bond in the phenalenyl dimer, the ligand bonding interaction between the iron porphyrin complex and the small molecule M ($M = O_2$ and CO), and the interactions in guanine-cytosine (G-C) base pair radicals. The basis set 6-31+G* is used for PLY₂, while 6-311+G* is used for the G-C base pair. The hybrid basis set, which is 6-31+G* for C, N, O, and H, while LanL2DZ for Fe, is used for [imidazole-iron-porphyrin]-M ($M = O_2$ and CO).

IV. RESULTS AND DISCUSSION

A. The pancake bond in the phenalenyl dimer

Phenalenyl (PLY) is an odd-alternant hydrocarbon π -radical with the high symmetry (D_{3h}). In the phenalenyl dimer (PLY₂), each neutral PLY contains one magnetic electron. The π - π stacking dimer is stabilized by the formation of a two-electron, 12-center (2e/12c) bond, often called the “pancake bond.”^{94–99} The experimental value of the singlet-triplet gap of PLY₂ is only 6.64 kcal/mol.⁹⁶ The ground state of the phenalenyl dimer is in the open shell singlet state. As for the physical origin of the pancake bond, Novoa *et al.* concluded that van der Waals interaction is the most important.⁹⁷ However, according to the work by Kertesz *et al.*, the pancake bond is dominated by the two singly occupied molecular orbitals (SOMO-SOMO) interaction, not the vdW interaction.⁹⁸

Figure 1 shows the optimized geometry and spin density of PLY₂ by ω B97X-D. The corresponding results of the other DFT functionals are shown in Table S1. D_c is the distance between the two central carbons of the PLY monomers, and \bar{D}_α is the average distance of six pairs of nearest α -carbons. The computed distances are close to the experimental data 3.2–3.3 Å by X-ray^{94–96} and the multireference average quadratic coupled cluster (MRAQCC) result of 3.104 Å by Kertesz *et al.*⁹⁸ According to the $\langle \hat{S}^2 \rangle$ values and spin densities of ω B97X-D and M05-2X, the unpaired α and β electrons are located at different monomers. However, TPSSh, B3LYP, and M06-2X improperly predict the pancake bond as the strong coupling in the close-shell singlet state. Consequently, only ω B97X-D and M05-2X are used for EDA calculations.

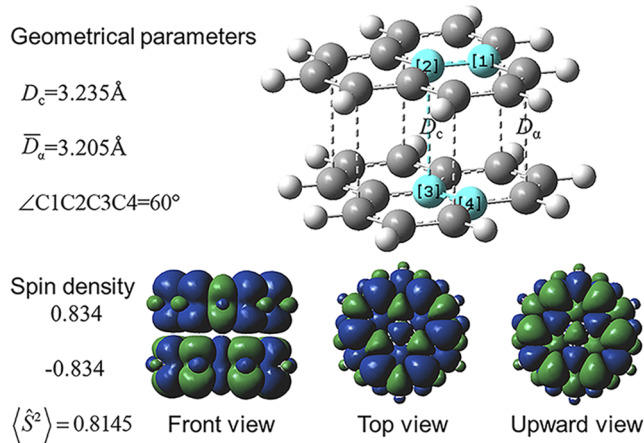


FIG. 1. Geometry and spin density distribution of the phenalenyl dimer (PLY_2) by $\omega\text{B97X-D}$.

Table I shows the GKS-EDA(WS) results in the equilibrium distance by M05-2X and $\omega\text{B97X-D}$. First, it is shown that the total interaction energies with zero point energy (ZPE) correction are close to the result of MRAQCC/6-31+G*, -11.5 kcal/mol,⁹⁸ and the experimental data, -9.5 kcal/mol.⁹⁵ The total interaction energy and the optimized geometry show the accuracy of broken symmetry DFT when appropriate functionals are applied. The NBO charges with α -spin orbitals and β -spin orbitals in Table S2 again demonstrate that, in the BS-UDFT calculations, different spins are located at different monomers.

It is found that the pancake bond is dominated by the correlation term. Electrostatic plays the secondary role, while polarization is close to zero. As a result, the electronic correlation is the most important in the pancake bond. The negligible value of the polarization term indicates that the orbital relaxation for the pancake bond is very small. It can be illustrated by the electron density difference map (EDDM) in Fig. 2. The EDDM of the BS- $\omega\text{B97X-D}$ in Fig. 2(a) is similar to the one of CASSCF(2,2) displayed in Fig. 2(c), showing the decrease in electronic density in the pancake bond. The active orbital in each PLY tends to stay away from each other with the SCF procedure, leading to the small orbital relaxation (polarization).

Without the broken symmetry scheme, KS-UDFT is unable to predict the pancake bond properly. The spin densities and NBO charges with α -spin orbitals and β -spin orbitals in Table S2 indicate that, according to KS-UDFT calculations, the dimer is in the

close-shell singlet state. The total interaction energy in GKS-EDA is smaller than the result of the high level MO method and the experimental data mentioned above. The polarization term in GKS-EDA is large and positive, showing that the orbital relaxation is repulsive. The improper polarization value is interpreted by the EDDM in Fig. 2(b). The EDDM by $\omega\text{B97X-D}$ is different from those of BS- $\omega\text{B97X-D}$ and CASSCF(2,2), showing the increase in the electron density between the two PLY molecules. It is shown that the broken symmetry scheme is necessary for the OSS type intermolecular interaction. As such, only the results of GKS-EDA(WS) are shown and discussed hereinafter.

The potential energy surfaces (PES) of PLY_2 along with the central C-C distance by M05-2X and $\omega\text{B97X-D}$ at the OSS and the triplet state (TS) are shown in Fig. 3. At the short distance less than 4.0 Å, the OSS interaction energy is lower than the TS one. At the long distance, the two states are degenerated. The singlet-triplet energy gaps ($\Delta E_{S-T} = E_{GS} - E_{TS}$, at each equilibrium distance, respectively), -10.7 kcal/mol by M05-2X, are similar to the result of -8.2 kcal/mol at the MRAQCC/6-31G* level.⁹⁸ It is shown that, for the whole PES, the total interactions of the two states are both controlled by the correlation and electrostatic terms. The polarization term is always small. The relative stability of the interaction in the OSS compared to that in the TS is mainly attributed to the correlation interaction.

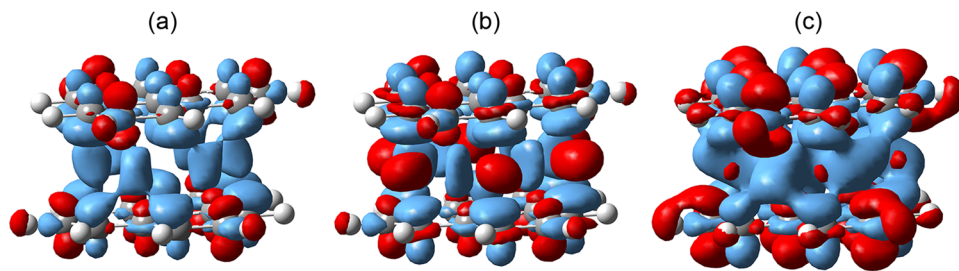
The PES of the rotation around the central C-C axis in the OSS and TS by M05-2X and $\omega\text{B97X-D}$ are displayed in Fig. 4. The global minimum of the OSS curve is at the angle of 60° , while the maximum point is at the angles of 30° and 90° . The curves are quite close to the MRAQCC one. The rotation barrier in the OSS, 18.80 kcal/mol, is close to the MRAQCC result, 16.7 kcal/mol.⁹⁸ The rotation barrier in the OSS is controlled by correlation and exchange repulsion, while that in the TS is mainly dominated by exchange repulsion. Therefore, the physical origins of the rotation barriers in the OSS and TS are quite different.

B. [Iron-porphyrin]-M interaction (M = O₂ and CO)

The iron porphyrin (FeP) is one of the important functional groups for electron transfer, oxygen transfer, and photosynthesis in biomolecules. The interactions between the iron porphyrin and the small molecule M (M = CO and O₂) in protein environments, which have long been the subject of interest in both theoretical and experimental studies, are investigated here. The imidazole (Im) group is used to model the axis residue ligand. The dielectric constant (ϵ) is set as 4.0 and 20.0 to model the protein environments, and 54.18 to model the blood environment.¹⁰⁰

TABLE I. GKS-EDA(WS) result and GKS-EDA result of PLY_2 in the equilibrium distances (kcal/mol).

DFT	ΔE^{ele}	ΔE^{exrep}	ΔE^{pol}	ΔE^{disp}	ΔE^{corr}	ΔE^{TOT}	$\Delta E^{\text{TOT}} + \text{ZPE}$
BS- $\omega\text{B97X-D}$	-11.11	34.92	-2.14	-15.98	-24.66	-18.98	-16.64
BS-M05-2X	-15.10	45.95	0.74		-44.70	-13.10	-11.46
$\omega\text{B97X-D}$	-11.11	36.53	21.86	-15.98	-40.60	-9.31	-6.97
M05-2X	-15.10	47.11	14.16		-53.77	-7.60	-5.96



The theoretical treatment for Im–FeP···O₂ is challenging for DFT. It has been pointed out in the literature that the ground state of Im–FeP···O₂ is an open shell singlet state, in which both Im–FeP and O₂ are triplet states in the complex.^{101–104} The key geometrical parameters and spin densities of Im–FeP···O₂ computed with

TPSSh are shown in Fig. 5, while the results with other functionals are shown in Table S3. It is shown that TPSSh, B3LYP, and ω B97X-D provide the accurate geometrical parameters, close to the experimental data. According to the $\langle \hat{S}^2 \rangle$ values and spin densities by the three functionals, α and β electrons are mainly located at

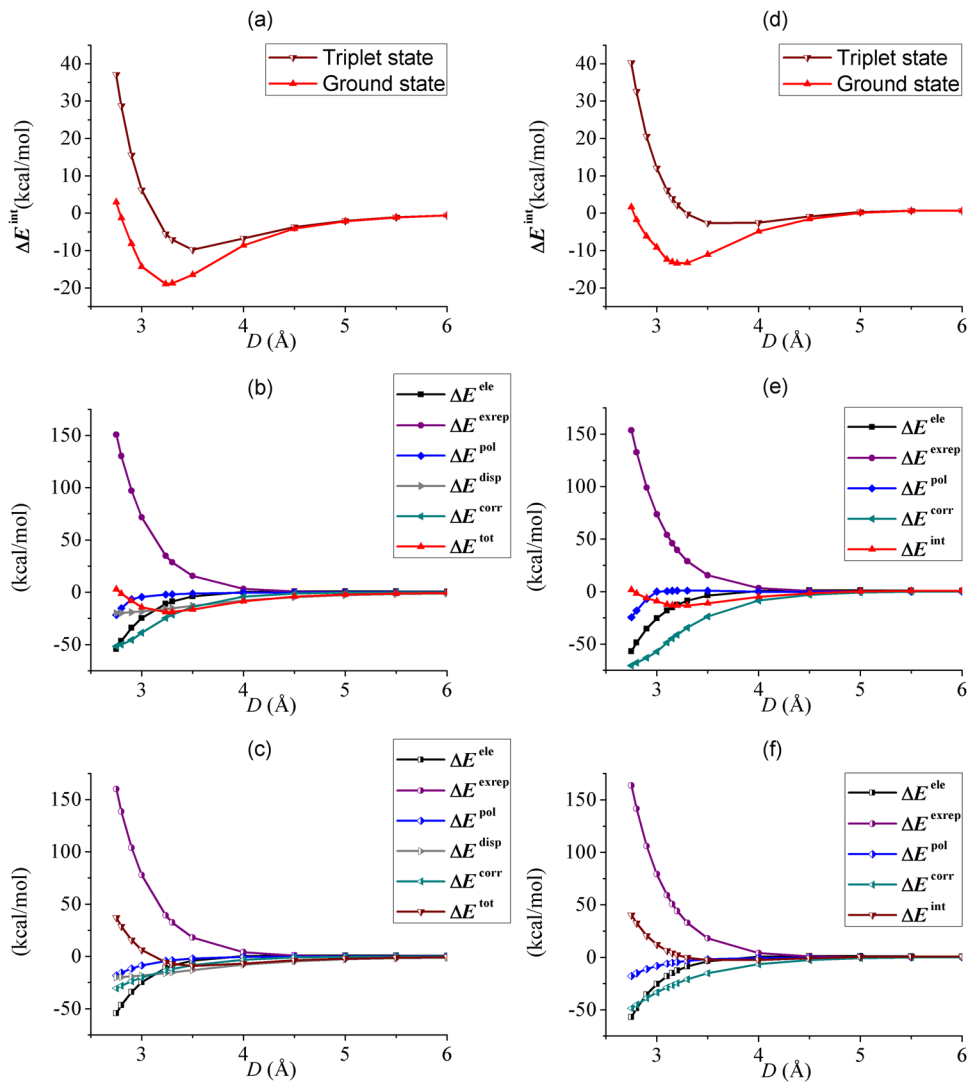


FIG. 3. Potential energy surfaces (PES) of PLY₂ along with the central C–C distance by ω B97X-D and M05-2X. (a) Total interaction energies in the triplet state and ground state by ω B97X-D; (b) GKS-EDA(BS) results in the ground state by ω B97X-D; (c) GKS-EDA(BS) results in the triplet state by ω B97X-D; (d) total interaction energies in the triplet state and ground state by M05-2X; (e) GKS-EDA(BS) results in the ground state by M05-2X; (f) GKS-EDA(BS) results in the triplet state by M05-2X.

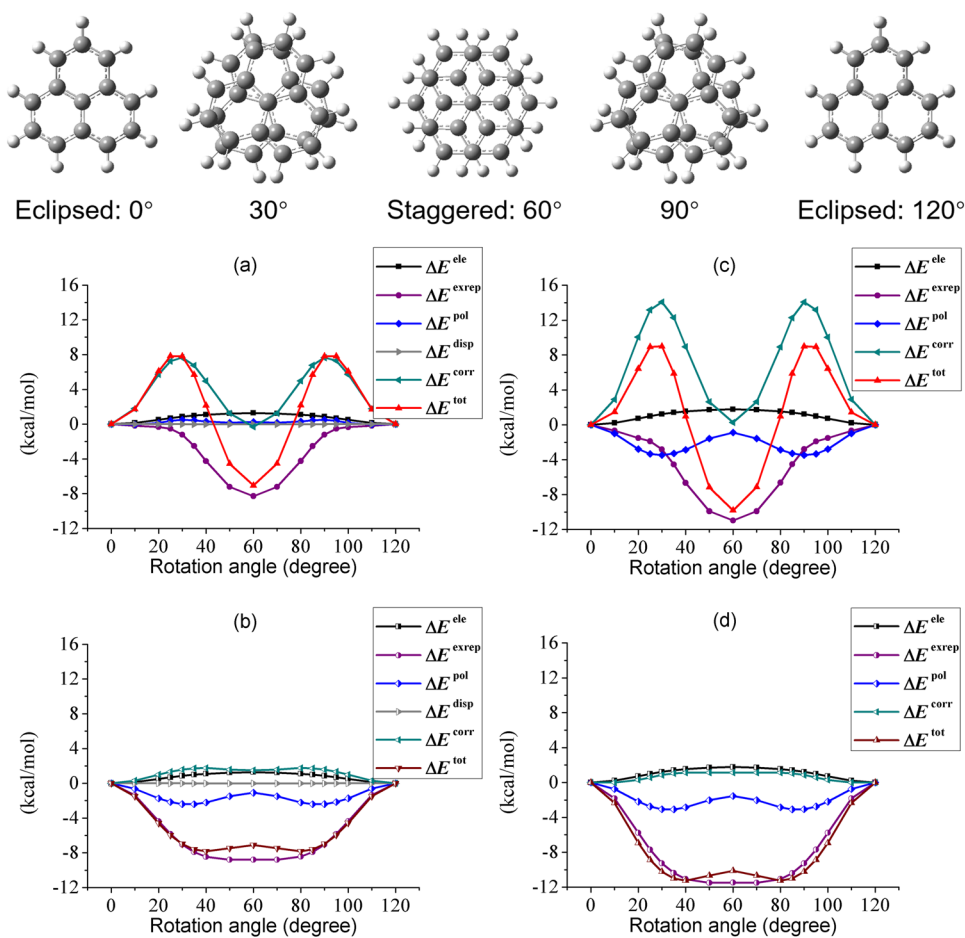


FIG. 4. GKS-EDA(BS) results of the rigid rotation scans of PLY₂ by ω B97X-D and M05-2X. (a) Ground state by ω B97X-D; (b) triplet state by ω B97X-D; (c) ground state by M05-2X; (d) triplet state by M05-2X. The dihedral angle of the eclipsed conformer is set as 0°.

Im-FeP and O₂, respectively, predicting the correct open shell singlet state. Then for GKS-EDA(BS) calculations, these three functionals are employed.

The GKS-EDA(BS) results for Im-FeP...O₂ with TPSSh are shown in Table II. The interaction energies with ZPE corrections range from -15.81 to -18.76 kcal/mol with the variation of ϵ values, compared to the TPSSh result in solution by Kepp *et al.*, -24.78 kcal/mol,¹⁰⁵ and the CASPT2 result by Novoa *et al.*, -14.9 kcal/mol.¹⁰⁶ The GKS-EDA(BS) results of B3LYP and ω B97X-D in Table S4 are similar to the TPSSh ones, showing the satisfactory accuracy of BS-UDFT for the Fe...O₂ bonding.

Among the individual terms, the correlation term is the most important, while the electrostatic term plays the secondary role. The polarization term is quite small, showing the weak covalency of the O₂ bonding. For instance, with $\epsilon = 54.18$, the correlation term is -73.70 kcal/mol, larger than the values of electrostatic and polarization, -51.70 and -6.83 kcal/mol, respectively. The negative desolvation term suggests that the solvent effect tends to enhance the O₂ ligand bonding. It agrees with the discussion of Watts *et al.*, which stated that the protein environment tends to enhance the O₂ bonding with the iron site.¹⁰⁷ It also accords with the variation of NBO

charges with the ϵ values, which indicates that Fe...O₂ becomes more polarized with the solvent effects. As can be seen from Table S4, the ω B97X-D and B3LYP results are similar to the TPSSh ones, showing that the correlation term is the largest contribution to the O₂ ligand bonding.

For Im-FeP...CO, the ground state is the close-shell singlet state. In Im-FeP...CO, Im-FeP is in the singlet state. Figure 6 displays the key geometrical parameters of Im-FeP...CO by TPSSh, while the results of the other functionals are shown in Table S5. As can be seen, the Fe...CO distance is shorter than the Fe...O₂ one, while the angle \angle Fe-C-O is almost 180°.

For Im-FeP...CO, $c = 0$, the GKS-EDA(BS) results are equal to the regular GKS-EDA ones. The GKS-EDA(BS) results for the Im-FeP...CO interaction in solvated environments with TPSSh are shown in Table II, and the results with B3LYP and ω B97X-D are shown in Table S6. The total interaction energy of Im-FeP...CO is insensitive to the variation of the ϵ value. With $\epsilon = 54.18$, the total interaction energies with ZPE corrections, -22.18, -21.33, and -31.87 kcal/mol by ω B97X-D, B3LYP, and TPSSh, respectively, are similar to the value of -19.6 kcal/mol by B3LYP and -32.1 kcal/mol by BP86.¹⁰⁸ Among the interaction terms,

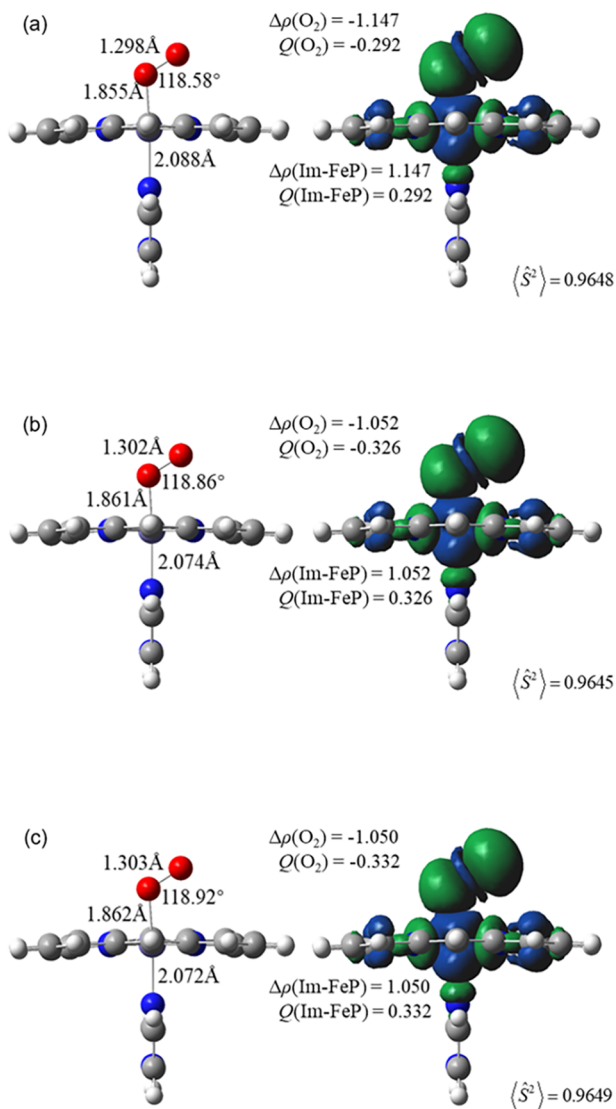


FIG. 5. Geometry, spin density ($\Delta\rho$), and NBO charge population (Q) of Im-FeP...O₂ by TPSSh. (a) $\epsilon = 4.0$; (b) $\epsilon = 20.0$; (c) $\epsilon = 54.18$.

electrostatic interaction is the largest, playing the most important role, while the polarization and correlation terms are also large. The large polarization term indicates the large covalency of the CO ligand bond. The desolvation term is very small, indicating that solvent environments are unable to alter the interaction. In summary, the nature of Im-FeP...CO is quite different from that of Im-FeP...O₂. The large total interaction energy of Im-FeP...CO compared to Im-FeP...O₂ can be mainly attributed to the strong polarization interaction.

C. Dehydrogenated Guanine-Cytosine base pair radicals

Dehydrogenated guanine-cytosine base pair radicals, which can be obtained by removing hydrogen atoms from the guanine-cytosine base pair, are important for understanding the mechanism and activity of the DNA damage.¹⁰⁹ If two hydrogen atoms are removed, there are two unpaired electrons in the dehydrogenated G-C radicals. The ground states of the G-C radicals are open shell singlet states. The interactions in the dehydrogenated base pair radicals have been explored extensively.^{110–113} Schaefer III and co-workers reported the possibility of formation of several open shell deprotonated guanine-cytosine (G-C) radicals.¹¹⁰ Chakrabarti *et al.* investigated the magnetic interactions in dehydrogenated G-C radicals.¹¹² The previous works focus on the magnetic coupling or the relative stability of various conformers. The physical origins of the base pair radical interactions compared to the original G-C base pair are still highly expected.

The ωB97X-D computed geometrical parameters and spin densities of the eight G-C base pair radicals in Chakrabarti's paper are shown in Fig. 7, where the abstracted hydrogen atoms are highlighted. Conformer VI is composed of the guanine diradical and cytosine, and the other conformers are formed by the guanine radical and the cytosine radical.

Among the five DFT functionals, ωB97X-D, M05-2X, and M06-2X provide the similar total interaction energies of the G-C base pair compared to the CCSD(T)/aug-cc-pVQZ value, -32.12 kcal/mol.¹³ The GKS-EDA(BS) results of the G-C radicals by ωB97X-D are displayed in Table III, and those by M05-2X and M06-2X are shown in Table S7.

Similar to that of the G-C base pair, the interactions in these G-C radicals are also controlled by the electrostatic and polarization interactions. This is because in these radicals, the three hydrogen

TABLE II. GKS-EDA(BS) results of Im-FeP...O₂ and Im-FeP...CO in solvated environments by TPSSh (kcal/mol).

	ϵ	ΔG^{ele}	ΔG^{exrep}	ΔG^{pol}	ΔG^{desol}	ΔG^{corr}	ΔG^{TOT}	$\Delta G^{\text{TOT}} + \text{ZPE}$
Im-FeP...O ₂	4.00	-51.95	119.58	-7.66	-4.49	-73.45	-17.97	-15.81
	20.00	-51.77	118.38	-6.82	-6.35	-73.84	-20.41	-18.33
	54.18	-51.70	118.07	-6.83	-6.70	-73.70	-20.85	-18.76
Im-FeP...CO	4.00	-75.94	154.86	-47.16	-0.26	-66.60	-35.11	-31.26
	20.00	-76.85	156.84	-47.64	-0.41	-67.22	-35.28	-31.80
	54.18	-76.97	157.08	-47.70	-0.44	-67.30	-35.33	-31.87

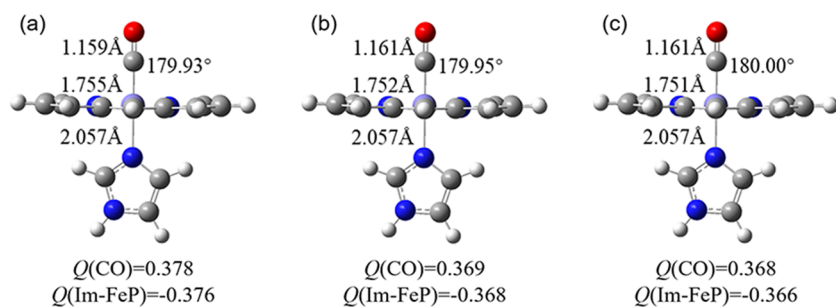


FIG. 6. Geometry and NBO charge population of Im-FeP...CO by TPSSh. (a) $\epsilon = 4.0$; (b) $\epsilon = 20.0$; (c) $\epsilon = 54.18$.

bonds are still retained. It is noticed that different from the previous two examples (PLY₂ and Im-FeP...O₂), the correlation interaction is not the most important in the radical interactions. According to their total interaction energies, the radicals can be divided into three

groups. The first group includes conformers I, V, and VII. As can be seen from Table III, their total interaction energies and the interaction terms are similar to those of the G-C base pair because the three hydrogen bonds in the G-C radicals are almost unchanged.

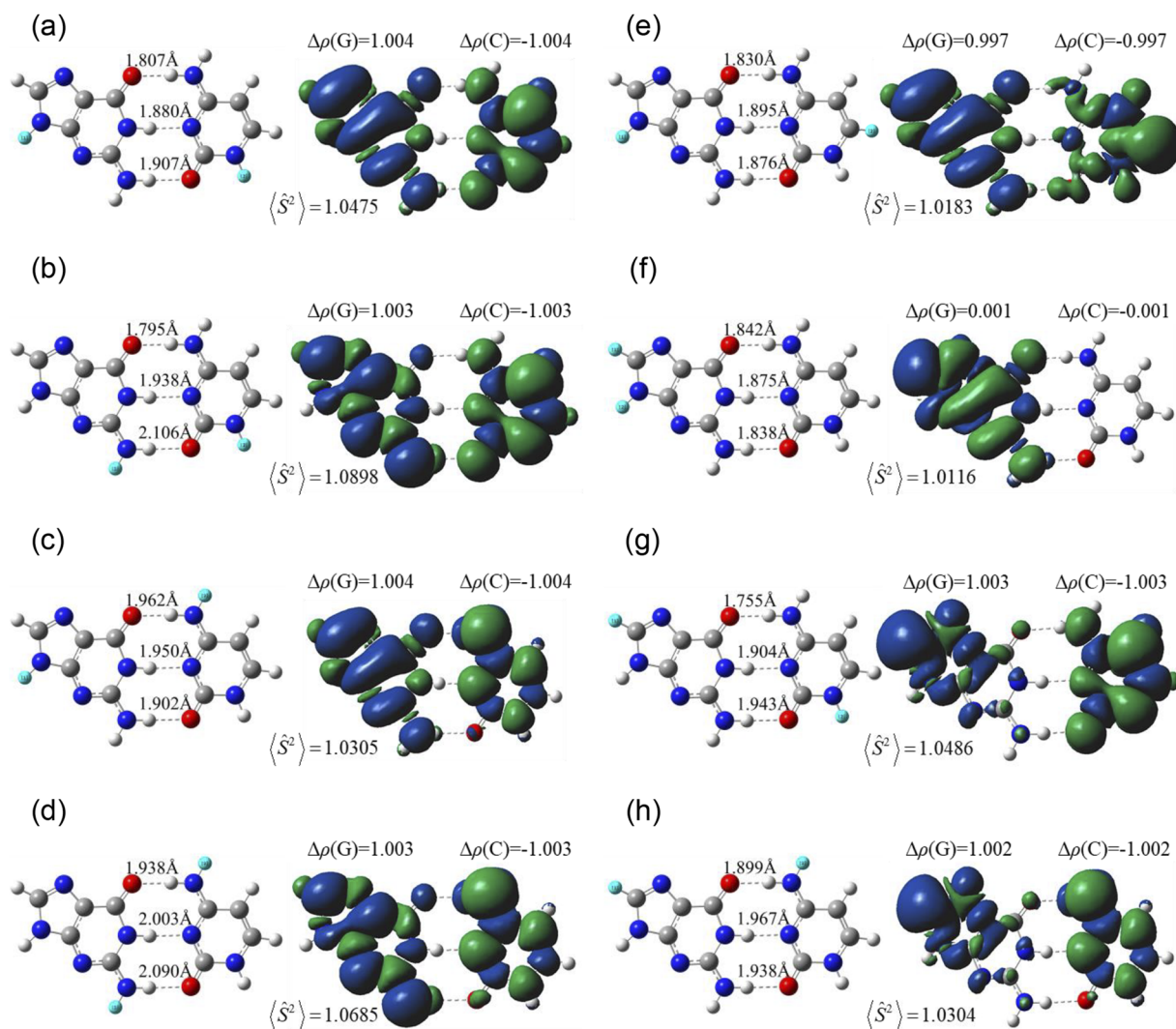


FIG. 7. Bond lengths of the triple hydrogen bonds and spin density distributions in the eight G-C base pairs (a)–(h) by ω B97X-D.

TABLE III. GKS-EDA(BS) results of the G-C base pair and the eight conformers of the dehydrogenated G-C base pairs by ω B97X-D (kcal/mol).

	ΔE^{ele}	ΔE^{exrep}	ΔE^{pol}	ΔE^{disp}	ΔE^{corr}	ΔE^{TOT}
G-C base pair	-43.34	41.65	-22.15	-3.42	-4.61	-31.87
Conformer I	-40.71	40.50	-20.48	-3.39	-6.91	-30.99
Conformer V	-41.88	39.72	-22.09	-3.41	-4.25	-31.91
Conformer VII	-41.16	41.47	-21.33	-3.39	-5.63	-30.06
Conformer II	-32.13	34.44	-17.24	-3.21	-4.76	-22.90
Conformer III	-32.78	31.83	-16.11	-3.19	-4.46	-24.73
Conformer IV	-25.08	27.00	-13.11	-3.02	-3.11	-17.33
Conformer VIII	-32.38	32.57	-16.55	-3.19	-3.47	-23.02
Conformer VI	-45.80	42.25	-23.59	-3.44	-4.71	-35.27

The second group involves conformers II, III, IV, and VIII. It can be seen that their total interaction energies are smaller than that of the G-C base pair. The electrostatic, exchange repulsion, and polarization terms in the four conformers are smaller than the corresponding values of the G-C base pair. It is shown that removing the hydrogen atoms from the functional groups in the G-C radicals leads to the large decrease in the total interaction energies.

The third group includes conformer VI. It is the interaction between a diradical and a close shell molecule. GKS-EDA(BS) shows the slightly enhanced total interaction energy compared to that of the G-C base pair. This is because after dehydrogenation, the functional groups become more positive, which leads to the weakening of the O(G) \cdots H-N(C) hydrogen bond and the strengthening of the N-H(G) \cdots N(C) and the N-H \cdots O(C) hydrogen bond. The GKS-EDA(BS) result shows that electrostatic and polarization in conformer VI mainly contribute to the increase in the total interaction energy compared to the base pair one.

The GKS-EDA(BS) results for the interactions of the G-C radicals in solvated environments are shown in Table S7. It is shown that the physical origin of the radical interactions in the solvated environment is similar to that in the gas phase discussed above.

V. CONCLUSION

In this paper, generalized Kohn-Sham energy decomposition analysis (GKS-EDA) is extended to the intermolecular interactions in molecular systems with open shell singlet states. The extension is based on the BS-UDFT calculations with a spin projection correction and thus named GKS-EDA(BS). GKS-EDA(BS) uses a linear combination of two independent energy calculations of single-determinant unrestricted spin configurations, i.e., broken-symmetry (BS) state and high-spin (HS) state, dividing the total interaction energy into electrostatic, exchange-repulsion, polarization, desolvation, correlation, and dispersion terms. For strong coupling between the unpaired electrons in each monomer, $\langle \hat{S}^2 \rangle = 0$, the GKS-EDA(BS) scheme will retreat to the regular GKS-EDA one.

Some points for the test examples are highlighted as follows:

1. The pancake bond in the phenalenyl dimer is dominated by the correlation interaction. The potential energy surfaces of the elongation for the central C-C distance and the rotation around the central C-C axis in the ground state are controlled by the correlation energy.
2. The physical origins of the ligand bonding interactions of CO and O₂ with the iron porphyrin complex are different. The ligand bonding of O₂ is dominated by the correlation and electrostatic interactions. Solvent effects tend to enhance the O₂ bonding interaction. In contrast, the CO bonding belongs to a typical ligand bond controlled by the electrostatic and polarization interactions.
3. The origin of the interactions in the dehydrogenated guanine-cytosine base pair radicals is the same as that of the guanine-cytosine base pair, controlled by electrostatic and polarization interactions. It is shown that the unpaired (magnetic) electrons in different monomers do not always result in the interactions with multireference characters if these electrons are not involved in the total interaction.

It must be stressed that the theoretical descriptions for these type of interactions are still challenging for DFT functionals. For example, M05-2X is good for the pancake bond but is bad for the Im-FeP \cdots O₂ interaction. It is reversed for B3LYP. It is suggested that testing calculations of DFT functionals are necessary for the interactions in open shell singlet systems.

Furthermore, the spin projection approximation, which is used in the current version of GKS-EDA(BS), does not include orbital angular momentum contributions explicitly. Bolvin and collaborators explicitly discuss the limitations of the neglect of the orbital angular momentum.^{78,80,81} Moreover, it is noticed that the polarization term is occasionally positive, for example, the value of 0.74 kcal/mol by M05-2X in Table I. It is because the current definition depends on the Yamaguchi correction, expressed as a linear combination of interaction terms in two states. Accidentally, with a certain DFT functional which provides a small $\langle \hat{S}^2 \rangle_{\text{BS}}$ value, the value of polarization in the BS state multiplied by (1 + c) can be

smaller than that in the HS state multiplied by c in absolute value, leading to the small and positive term. Further works can be devoted to improving the accuracy of GKS-EDA(BS).

SUPPLEMENTARY MATERIAL

See the [supplementary material](#) associated with this article.

ACKNOWLEDGMENTS

This project was supported by the National Natural Science Foundation of China (Grant Nos. 21573176 and 21733008), the New Century Excellent Talents in Fujian Province University, and the Fundamental Research Funds for the Central Universities (Grant No. 20720190046).

REFERENCES

- ¹K. Kitaura and K. Morokuma, *Int. J. Quantum Chem.* **10**, 325 (1976).
- ²K. Morokuma, *Acc. Chem. Res.* **10**, 294 (1977).
- ³T. Ziegler and A. Rauk, *Theor. Chim. Acta* **46**, 1 (1977).
- ⁴P. S. Bagus, K. Hermann, and C. W. Bauschlicher, Jr., *J. Chem. Phys.* **80**, 4378 (1984).
- ⁵S. Rybak, B. Jeziorski, and K. Szalewicz, *J. Chem. Phys.* **95**, 6576 (1991).
- ⁶B. Jeziorski, R. Moszynski, and K. Szalewicz, *Chem. Rev.* **94**, 1887 (1994).
- ⁷W. Chen and M. S. Gordon, *J. Phys. Chem.* **100**, 14316 (1996).
- ⁸T. A. Wesolowski, Y. Ellinger, and J. Weber, *J. Chem. Phys.* **108**, 6078 (1998).
- ⁹Y. Mo, J. Gao, and S. D. Peyerimhoff, *J. Chem. Phys.* **112**, 5530 (2000).
- ¹⁰D. G. Fedorov and K. Kitaura, *J. Comput. Chem.* **28**, 222 (2007).
- ¹¹R. Z. Khalilullin, E. A. Cobas, R. C. Lochan, A. T. Bell, and M. Head-Gordon, *J. Phys. Chem. A* **111**, 8753 (2007).
- ¹²M. P. Mitoraj, A. Michalak, and T. Ziegler, *J. Chem. Theory Comput.* **5**, 962 (2009).
- ¹³P. Su and H. Li, *J. Chem. Phys.* **131**, 014102 (2009).
- ¹⁴Q. Wu, P. W. Ayers, and Y. Zhang, *J. Chem. Phys.* **131**, 164112 (2009).
- ¹⁵P. Su, H. Liu, and W. Wu, *J. Chem. Phys.* **137**, 034111 (2012).
- ¹⁶P. Su, Z. Jiang, Z. Chen, and W. Wu, *J. Phys. Chem. A* **118**, 2531 (2014).
- ¹⁷P. Su, Z. Chen, and W. Wu, *Chem. Phys. Lett.* **635**, 250 (2015).
- ¹⁸P. Su, H. Chen, and W. Wu, *Sci. China Chem.* **59**, 1025 (2016).
- ¹⁹X. Chang, P. Su, and W. Wu, *Chem. Phys. Lett.* **610-611**, 246 (2014).
- ²⁰W. Gao, Y. Tian, and X. Xuan, *J. Mol. Graph. Model.* **60**, 118 (2015).
- ²¹Q. Gu, Z. Tang, P. Su, W. Wu, Z. Yang, C. O. Trindle, and J. L. Knee, *J. Chem. Phys.* **145**, 051101 (2016).
- ²²C. Yuan, P. An, J. Chen, Z. Luo, and J. Yao, *Sci. China Chem.* **59**, 1270 (2016).
- ²³C. Yuan, H. Wu, M. Jia, P. Su, Z. Luo, and J. Yao, *Phys. Chem. Chem. Phys.* **18**, 29249 (2016).
- ²⁴Q. Gu, D. Shen, Z. Tang, W. Wu, P. Su, Y. Xia, Z. Yang, and C. O. Trindle, *Phys. Chem. Chem. Phys.* **19**, 14238 (2017).
- ²⁵Q. Gu, P. Su, Y. Xia, Z. Yang, C. O. Trindle, and J. L. Knee, *Phys. Chem. Chem. Phys.* **19**, 24399 (2017).
- ²⁶Z. Liu, C. O. Trindle, Q. Gu, W. Wu, and P. Su, *Phys. Chem. Chem. Phys.* **19**, 25260 (2017).
- ²⁷R. L. T. Parreira, E. J. Nassar, E. H. da Silva, L. A. Rocha, P. A. de. S. Bergamo, C. M. A. Ferreira, T. Kar, D. E. P. Fonseca, D. F. Coimbra, and G. F. Caramori, *J. Lumin.* **182**, 137 (2017).
- ²⁸H. Zhao and L. Du, *Environ. Sci.: Processes Impacts* **19**, 65 (2017).
- ²⁹P. An, L. Kang, Z. Tang, P. Su, and Z. Luo, *Chin. Chem. Lett.* **29**, 361 (2018).
- ³⁰Z.-F. Li, X.-P. Yang, H.-X. Li, and G.-F. Zuo, *Nanomaterials* **8**, 685 (2018).
- ³¹D. Shen, P. Su, and W. Wu, *Phys. Chem. Chem. Phys.* **20**, 26126 (2018).
- ³²X. Sheng, X. Jiang, H. Zhao, D. Wan, Y. Liu, C. A. Ngwenya, and L. Du, *Spectrochim. Acta A* **198**, 239 (2018).
- ³³A. L. Amorim, M. M. Peterle, A. Guerreiro, D. F. Coimbra, R. S. Heying, G. F. Caramori, A. L. Braga, A. J. Bortoluzzi, A. Neves, G. J. L. Bernardes, and R. A. Peralta, *Dalton Trans.* **48**, 5574 (2019).
- ³⁴K. F. Andriani, G. Heinzelmann, and G. F. Caramori, *J. Phys. Chem. B* **123**, 457 (2019).
- ³⁵X. Sheng, X. Song, C. A. Ngwenya, Y. Wang, X. Gao, and H. Zhao, *Struct. Chem.* **30**, 1415 (2019).
- ³⁶M. Xie and W. Lu, *Dalton Trans.* **48**, 1275 (2019).
- ³⁷M. Abe, *Chem. Rev.* **113**, 7011 (2013).
- ³⁸M. Nakano and B. Champagne, *Wiley Interdiscip. Rev.: Comput. Mol. Sci.* **6**, 198 (2016).
- ³⁹H. Szatylowicz, T. M. Krygowski, M. Solà, M. Palusiak, J. Dominikowska, O. A. Stasyuk, and J. Poater, *Theor. Chem. Acc.* **134**, 35 (2015).
- ⁴⁰K. Patkowski, P. S. Zuchowski, and D. G. A. Smith, *J. Chem. Phys.* **148**, 164110 (2018).
- ⁴¹J. M. Waldrop and K. Patkowski, *J. Chem. Phys.* **150**, 074109 (2019).
- ⁴²F. Bernardi and M. A. Robb, *Mol. Phys.* **48**, 1345 (1983).
- ⁴³F. Bernardi, A. Bottoni, and M. A. Robb, *Theor. Chem. Acta* **64**, 259 (1984).
- ⁴⁴C. W. Bauschlicher, Jr., P. S. Bagus, C. J. Nelin, and B. O. Roos, *J. Chem. Phys.* **85**, 354 (1986).
- ⁴⁵T. M. Cardozo and M. A. C. Nascimento, *J. Chem. Phys.* **130**, 104102 (2009).
- ⁴⁶D. Danovich, S. Shaik, F. Neese, J. Echeverría, G. Aullón, and S. Alvarez, *J. Chem. Theory Comput.* **9**, 1977 (2013).
- ⁴⁷Y. Zhang, S. Chen, F. Ying, P. Su, and W. Wu, *J. Phys. Chem. A* **122**, 5886 (2018).
- ⁴⁸L. Noddeman, *J. Chem. Phys.* **74**, 5737 (1981).
- ⁴⁹F. Neese, *J. Phys. Chem. Solids* **65**, 781 (2004).
- ⁵⁰N. N. Nair, E. Schreiner, R. Pollet, V. Staemmler, and D. Marx, *J. Chem. Theory Comput.* **4**, 1174 (2008).
- ⁵¹D. Bovi and L. Guidoni, *J. Chem. Phys.* **137**, 114107 (2012).
- ⁵²T. Lovell, J. E. McGrady, R. Stranger, and S. A. Macgregor, *Inorg. Chem.* **35**, 3079 (1996).
- ⁵³E. Coulaud, N. Guihéry, J.-P. Malrieu, D. Hagebaum-Reignier, D. Siri, and N. Ferré, *J. Chem. Phys.* **137**, 114106 (2012).
- ⁵⁴E. Coulaud, J.-P. Malrieu, N. Guihéry, and N. Ferré, *J. Chem. Theory Comput.* **9**, 3429 (2013).
- ⁵⁵D. S. Levine and M. Head-Gordon, *Proc. Natl. Acad. Sci. U. S. A.* **114**, 12649 (2017).
- ⁵⁶R. G. Parr and W. Yang, *Density Functional Theory of Atoms and Molecules* (Oxford University Press, New York, 1989).
- ⁵⁷P. Hohenberg and W. Kohn, *Phys. Rev.* **136**, B864 (1964).
- ⁵⁸W. Kohn and L. J. Sham, *Phys. Rev.* **140**, a1133 (1965).
- ⁵⁹A. Seidl, A. Görling, P. Vogl, J. A. Majewski, and M. Levy, *Phys. Rev. B* **53**, 3764 (1996).
- ⁶⁰S. Grimme, *J. Comput. Chem.* **25**, 1463 (2004).
- ⁶¹V. Barone and M. Cossi, *J. Phys. Chem. A* **102**, 1995 (1998).
- ⁶²M. Cossi, N. Rega, G. Scalmani, and V. Barone, *J. Comput. Chem.* **24**, 669 (2003).
- ⁶³E. Cancès and B. Mennucci, *J. Chem. Phys.* **109**, 249 (1998).
- ⁶⁴E. Cancès, B. Mennucci, and J. Tomasi, *J. Chem. Phys.* **109**, 260 (1998).
- ⁶⁵M. Cossi and V. Barone, *J. Chem. Phys.* **109**, 6246 (1998).
- ⁶⁶B. Mennucci, R. Cammi, and J. Tomasi, *J. Chem. Phys.* **110**, 6858 (1999).
- ⁶⁷P. Su and H. Li, *J. Chem. Phys.* **130**, 074109 (2009).
- ⁶⁸P.-O. Löwdin, *Phys. Rev.* **97**, 1474 (1955).
- ⁶⁹P.-O. Löwdin, *Phys. Rev.* **97**, 1490 (1955).
- ⁷⁰M. E. Lines, *J. Chem. Phys.* **55**, 2977 (1971).
- ⁷¹L. Noddeman and E. R. Davidson, *Chem. Phys.* **109**, 131 (1986).
- ⁷²K. Yamaguchi, Y. Takahara, and T. Fueno, in *Applied Quantum Chemistry*, edited by V. H. Smith, Jr., H. F. Schaefer III, and K. Morokuma (D. Reidel Publishing Company, Dordrecht, Holland, 1986), pp. 155–184.
- ⁷³J. Baker, *J. Chem. Phys.* **91**, 1789 (1989).
- ⁷⁴K. Yamaguchi, M. Okumura, K. Takada, and S. Yamanaka, *Int. J. Quantum Chem.* **48**, 501 (1993).

- ⁷⁵S. Yamanaka, T. Kawakami, H. Nagao, and K. Yamaguchi, *Chem. Phys. Lett.* **231**, 25 (1994).
- ⁷⁶C. J. Cramer, F. J. Dulles, D. J. Giesen, and J. Almlöf, *Chem. Phys. Lett.* **245**, 165 (1995).
- ⁷⁷A. A. Ovchinnikov and J. K. Labanowski, *Phys. Rev. A* **53**, 3946 (1996).
- ⁷⁸H. Bolvin, *Chemphyschem* **7**, 1575 (2006).
- ⁷⁹A. M. Mak, K. V. Lawler, and M. Head-Gordon, *Chem. Phys. Lett.* **515**, 173 (2011).
- ⁸⁰F. Gendron, D. Páez-Hernández, F. P. Notter, B. Pritchard, H. Bolvin, and J. Autschbach, *Chem. Eur. J.* **20**, 7994 (2014).
- ⁸¹C. Y. Chow, H. Bolvin, V. E. Campbell, R. Guillot, J. W. Kampf, W. Wernsdorfer, F. Gendron, J. Autschbach, V. L. Pecoraro, and T. Mallah, *Chem. Sci.* **6**, 4148 (2015).
- ⁸²N. Ferré, N. Guihéry, and J.-P. Malrieu, *Phys. Chem. Chem. Phys.* **17**, 14375 (2015).
- ⁸³A. J. Cohen, D. J. Tozer, and N. C. Handy, *J. Chem. Phys.* **126**, 214104 (2007).
- ⁸⁴M. W. Schmidt, K. K. Baldridge, J. A. Boatz, S. T. Elbert, M. S. Gordon, J. H. Jensen, S. Koseki, N. Matsunaga, K. A. Nguyen, S. Su, T. L. Windus, M. Dupuis, and J. A. Montgomery, Jr., *J. Comput. Chem.* **14**, 1347 (1993).
- ⁸⁵S. F. Boys and F. Bernardi, *Mol. Phys.* **19**, 553 (1970).
- ⁸⁶A. D. Becke, *J. Chem. Phys.* **98**, 5648 (1993).
- ⁸⁷J.-D. Chai and M. Head-Gordon, *Phys. Chem. Chem. Phys.* **10**, 6615 (2008).
- ⁸⁸J. Tao, J. P. Perdew, V. N. Staroverov, and G. E. Scuseria, *Phys. Rev. Lett.* **91**, 14601 (2003).
- ⁸⁹Y. Zhao, N. E. Schultz, and D. G. Truhlar, *J. Chem. Theory Comput.* **2**, 364 (2006).
- ⁹⁰Y. Zhao and D. G. Truhlar, *Theor. Chem. Acc.* **120**, 215 (2008).
- ⁹¹M. J. Frisch, G. W. Trucks, and H. B. Schlegel *et al.*, GAUSSIAN 09, Revision E.01, Gaussian, Inc., Wallingford, CT, 2013.
- ⁹²E. D. Glendening, A. E. Reed, J. E. Carpenter, and F. Weinhold, NBO version 3.1.
- ⁹³A. K. Rappe, C. J. Casewit, K. S. Colwell, W. A. Goddard, and W. M. Skiff, *J. Am. Chem. Soc.* **114**, 10024 (1992).
- ⁹⁴K. Goto, T. Kubo, K. Yamamoto, K. Nakasuiji, K. Sato, D. Shiomi, T. Takui, M. Kubota, T. Kobayashi, K. Yakusi, and J. Ouyang, *J. Am. Chem. Soc.* **121**, 1619 (1999).
- ⁹⁵D. Small, V. Zaitsev, Y. Jung, S. V. Rosokha, M. Head-Gordon, and J. K. Kochi, *J. Am. Chem. Soc.* **126**, 13850 (2004).
- ⁹⁶S. Suzuki, Y. Morita, K. Fukui, K. Sato, D. Shiomi, T. Takui, and K. Nakasuiji, *J. Am. Chem. Soc.* **128**, 2530 (2006).
- ⁹⁷F. Mota, J. S. Miller, and J. J. Novoa, *J. Am. Chem. Soc.* **131**, 7699 (2009).
- ⁹⁸Z.-h. Cui, H. Lischka, H. Z. Beneberu, and M. Kertesz, *J. Am. Chem. Soc.* **136**, 5539 (2014).
- ⁹⁹Z. Mou, Y.-H. Tianb, and M. Kertesz, *Phys. Chem. Chem. Phys.* **19**, 24761 (2017).
- ¹⁰⁰M. Martinez-Burdalo, A. Martin, M. Anguiano, and R. Villar, *Phys. Med. Biol.* **50**, 4125 (2005).
- ¹⁰¹D. S. McClure, *Radiat. Res. Suppl.* **2**, 218 (1960).
- ¹⁰²B. D. Olafson and W. A. Goddard III, *Proc. Natl. Acad. Sci. U. S. A.* **74**, 1315 (1977).
- ¹⁰³H. Chen, M. Ikeda-Saito, and S. Shaik, *J. Am. Chem. Soc.* **130**, 14778 (2008).
- ¹⁰⁴V. E. J. Berryman, R. J. Boyd, and E. R. Johnson, *J. Chem. Theory Comput.* **11**, 3022 (2015).
- ¹⁰⁵K. P. Kepp and P. Dasmeh, *J. Phys. Chem. B* **117**, 3755 (2013).
- ¹⁰⁶J. Ribas-Ariño and J. J. Novoa, *Chem. Commun.* **2007**, 3160.
- ¹⁰⁷M.-S. Liao, M.-J. Huang, and J. D. Watts, *J. Phys. Chem. B* **117**, 10103 (2013).
- ¹⁰⁸M. Radoń and K. Pierloot, *J. Phys. Chem. A* **112**, 11824 (2008).
- ¹⁰⁹S. Steenken, *Chem. Rev.* **89**, 503 (1989).
- ¹¹⁰M. C. Lind, P. P. Bera, N. A. Richardson, S. E. Wheeler, and H. F. Schaefer III, *Proc. Natl. Acad. Sci. U. S. A.* **103**, 7554 (2006).
- ¹¹¹S. Kim, M. C. Lind, and H. F. Schaefer III, *J. Phys. Chem. B* **112**, 3545 (2008).
- ¹¹²P. Seal, P. C. Jha, H. Ågren, and S. Chakrabarti, *Chem. Phys. Lett.* **465**, 285 (2008).
- ¹¹³M. Wang, J. Zhao, L. Zhang, X. Su, H. Su, and Y. Bu, *Chem. Phys. Lett.* **619**, 223 (2015).